Regimes of expansion of a collisional plasma into a vacuum

C. Thaury, P. Mora, J. C. Adam, and A. Héron

Citation: Physics of Plasmas **16**, 093104 (2009); doi: 10.1063/1.3206940
View online: http://dx.doi.org/10.1063/1.3206940
View Table of Contents: http://scitation.aip.org/content/aip/journal/pop/16/9?ver=pdfcov
Published by the AIP Publishing

Regimes of expansion of a collisional plasma into a vacuum

C. Thaury, P. Mora, J. C. Adam, and A. Héron
Centre de Physique Théorique, Ecole Polytechnique, CNRS, 91128 Palaiseau, France

(Received 26 May 2009; accepted 28 July 2009; published online 3 September 2009)

The effect of elastic Coulomb collisions on the one-dimensional expansion of a plasma slab is studied in the classical limit, using an electrostatic particle-in-cell code. Two regimes of interest are identified. For a collision rate of few hundreds of the inverse of the expansion characteristic time τ_e, the electron distribution function remains isotropic and Maxwellian with a homogeneous temperature, during all the expansion. In this case, the expansion can be approached by a three-dimensional version of the hybrid model developed by Mora [P. Mora, Phys. Rev. E **72**, 056401 (2005)]. When the collision rate becomes somewhat greater than $10^4\tau_e^{-1}$, the plasma is divided in two parts: an inner part which expands adiabatically as an ideal gas and an outer part which undergoes an isothermal expansion. © *2009 American Institute of Physics*.
[doi:10.1063/1.3206940]

I. INTRODUCTION

In the past decade, several experiments have demonstrated that high-quality beams of energetic ions can be generated by laser-plasma interaction.[1–6] Diverse models have been proposed to explain these observations.[7–10] The most frequently used assumes that ions are accelerated by an electrostatic field created at the plasma-vacuum interface by fast electrons.[7] These electrons, which have absorbed a large part of the laser energy during the interaction, form at the surface of the plasma a cloud of hot electrons, spreading on a few Debye lengths. The charge separation field thus created pulls ions toward vacuum, and transfers progressively the energy from the electrons to the ions.

Since 1966 and the pioneering work of Gurevitch,[11] the one-dimensional (1D) collisionless expansion of a plasma into a vacuum has been thoroughly studied theoretically.[12–21] These works provide a very accurate description of a purely 1D expansion, but they totally neglect the coupling between the longitudinal and transverse directions. Coulomb collisions are one potential source of such a coupling. Indeed, while the electron longitudinal velocities decrease during the expansion, collisions tend, for example, to redistribute the energy and isotropize the electron distribution.

Actually, Coulomb collision can influence the expansion of a fully ionized plasma through several effects, depending on the initial electron-electron basic collision frequency

$$\nu_0 = \frac{n_{e0}e^4 \ln \Lambda}{8\pi\sqrt{2}\epsilon_0^2 m_e^{1/2}(k_B T_{e0})^{3/2}}, \tag{1}$$

where $\ln \Lambda$ is the Coulomb logarithm,[22,23] n_{e0} is the electron initial density, m_e is the electron mass, and T_{e0} the initial electron temperature. For moderate frequencies, electron-electron and electron-ion collisions tend to maintain the electron distribution function isotropic and Maxwellian during all the expansion, whereas electrons and ions exchange very little energy. As ν_0 increases, electrons start to deliver a part of their energy to ions via collisions. If this process is sufficiently efficient, electron and ion temperatures can be perfectly equilibrated during the whole expansion. Finally, for very high collision rates, the electron mean free path can become much smaller than the temperature gradient scale length, leading to an adiabatic expansion. The characteristic times of these different processes are derived in Sec. II. Sections III and IV are then devoted to a detailed analysis of the Maxwellian-isotropic and adiabatic regimes.

II. CHARACTERISTIC FREQUENCIES

A. PIC code

To study the influence of Coulomb collisions on plasma expansion, we performed particle-in-cell (PIC) simulations, with a 1D3V, nonrelativistic and purely electrostatic code. Electron-electron, electron-ion, and ion-ion binary collisions are treated using the Monte Carlo method developed by Nanbu.[24] At each time step and in every cell, macroparticles are randomly combined by pairs.[25] Collisions between paired particles are then treated, using a cumulative scattering angle that simulates a succession of small-angle binary collisions.[22] This angle is a function of the collision frequency ν. It is calculated, for each pair of colliding macroparticles, by taking into account the dependency of ν on the particles relative velocity $\boldsymbol{v}_r$ ($\nu \propto 1/|\boldsymbol{v}_r|^3$). Note that for simplicity, the Coulomb logarithm is kept constant.

Since collisions tend to redistribute the energy of the system, we have to consider initial conditions with various ratios $T_{e0}^{\perp}/T_{e0}^{\parallel}$ and T_{i0}/T_{e0}, where $T_{e0}^{\parallel}$ and $T_{e0}^{\perp}$ are, respectively, the longitudinal and transverse initial electron temperatures, and $T_{e0}=(T_{e0}^{\parallel}+2T_{e0}^{\perp})/3$ and $[T_{i0}=(T_{i0}^{\parallel}+2T_{i0}^{\perp})/3]$ the initial electron (ion) total temperatures. However, to simplify the comparisons between the different parts of this article, the total thermal energy $T_0=(T_{e0}+T_{i0})/2$ is kept constant. Besides, all ion velocities are normalized to $c_{s0}=(6Zk_BT_0/m_i)^{1/2}$, i.e., to the ion acoustic velocity corresponding to the ideal collisionless case where electrons have been heated only in the longitudinal direction, with $T_{i0}=0$ and $T_{e0}^{\parallel}=6T_0$.

At the beginning of the simulations, the ions occupy a slab of half-thickness $L_0=20\lambda_{D0}$, where λ_{D0}

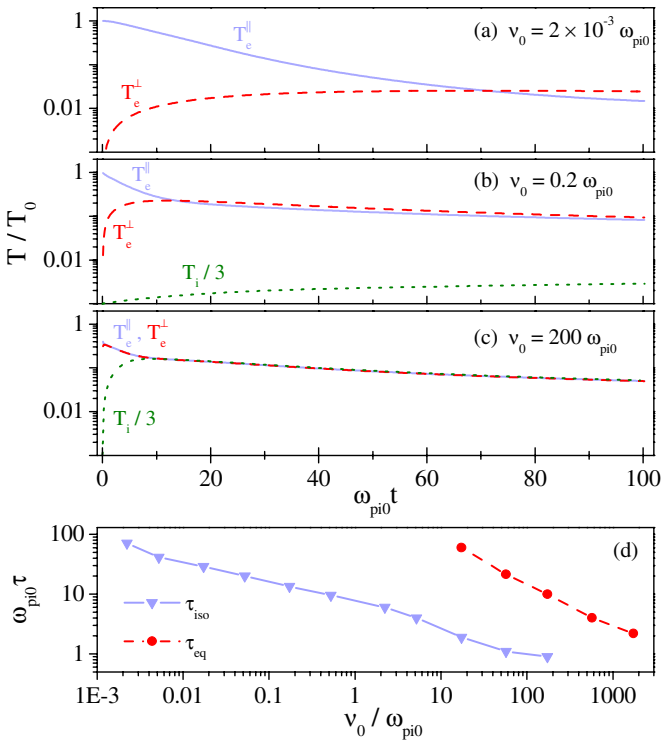

FIG. 1. (Color online) Relaxation of electron and ion temperatures. [(a)–(c)] Evolution in time of the transverse and longitudinal components of the electron mean temperature, and of the ion mean temperatures [(b) and (c)], for $\nu_0=2\times10^{-3}\omega_{pi0}$ (a), $\nu_0=0.2\omega_{pi0}$ (b), and $\nu_0=200\omega_{pi0}$ (c). (d) Variation of the electron isotropization time τ_{iso} and of the electron-ion thermal equilibration time τ_{eq}, as a function of the collision frequency.

$=(6\epsilon_0 m_e k_B T_0/n_{e0}e^2)^{1/2}$. Electrons are initially in Maxwell–Boltzmann equilibrium with the self consistent electrostatic potential with a Debye sheath in vacuum on both sides. The mass ratio is $m_e/m_i=1836$ with $Z=1$. The code is running with a time step of $\Delta t=0.01\omega_{pe}^{-1}$, where $\omega_{pe}=(n_{e0}e^2/m_e\epsilon_0)^{1/2}$ is the electron plasma frequency. Note that such a low time step is required to resolve the highest collisions frequencies considered. The simulation box is about $10^4\Delta x$, with $\Delta x=0.2\lambda_{D0}$, and there are 2×10^5 particles in each mesh.

B. Relaxation processes

One of the main effects of Coulomb collisions is to redistribute the energy of the system, in order to isotropize and equilibrate the electron and ion temperatures. A precise analysis of the dynamics of this redistribution is essential, since it can strongly affect the expansion. Indeed, collisions can, for instance, transfer a part of the electron momentum from the longitudinal to the transverse directions, limiting the expansion at its earliest stages, and then transfer it back to the longitudinal direction, enhancing the expansion on the long times. The aim of this section is to determine the characteristic frequencies of these transfers.

1. Temperature isotropization

We focus first on the isotropization of the electron temperature. Figure 1(a) shows the time evolution of its transverse and longitudinal components, for $\nu_0=2\times10^{-3}\omega_{pi0}$, $T_{e0}^{\parallel}=6T_0$, $T_{e0}^{\perp}=0$, and $T_{e0}/T_{i0}=1000$. These initial conditions correspond to an ideal case, where electrons have been exclusively accelerated along the longitudinal direction. We observe that $T_e^{\parallel}$ strongly decreases from the beginning of the expansion, as electrons transfer a part of their longitudinal momentum to ions through the charge separation field, and a part to the transverse directions through collisions. Accordingly, as $T_e^{\parallel}$ decreases, $T_e^{\perp}$ increases up to the time $\tau_{iso}\approx70\omega_{pi0}^{-1}$, where $T_e^{\perp}=T_e^{\parallel}$. At that time, more than 90% of the initial energy has been transferred to accelerated ions. Then $T_e^{\parallel}$ and $T_e^{\perp}$ diminish together, as electrons cool down during the expansion. We remark that after τ_{iso}, $T_e^{\perp}>T_e^{\parallel}$. This indicates that collisions are not efficient enough to counterbalance "instantaneously" the cooling down.

To evaluate the isotropization characteristic frequency, we must consider the contributions of both electron-electron and electron-ion collisions. For $Z=1$, the macroscopic relaxation rates corresponding to these two processes are equal and the total relaxation rate for $T_e^{\perp}\approx T_e^{\parallel}$ is $\nu_{iso}^{elec}=(16/5\sqrt{2\pi})\nu_0$.[25] To estimate the ability of collisions to maintain an isotropic distribution during the expansion, this rate must be compared to the inverse of the expansion characteristic time of an isotropic plasma, $1/\tau_e=T_e^{-1}|\partial T_e/\partial t|=(2/3)c_s/L$, where $c_s=c_{s0}/\sqrt{3}$ is the ion acoustic velocity in an isotropic, nonequilibrated plasma (see Sec. III B). Actually, the isotropic regime is entered when $\nu_{iso}^{elec}\gg1/\tau_e$, i.e., when

$$\nu_0 \gg \nu_0^{is}=0.3\frac{c_{s0}}{L}. \tag{2}$$

For $L=20\lambda_{D0}$, this leads to $\nu_0\gg0.015\omega_{pi0}$. Accordingly, Fig. 1(b) shows that, for $\nu_0=0.2\omega_{pi0}$, $T_e^{\perp}\approx T_e^{\parallel}$ for all $t>\tau_{iso}$.

This figure also suggests that, for $T_{e0}^{\perp}\ll T_{e0}^{\parallel}$ and $\nu_0\gg\nu_0^{is}$, the expansion can be separated in two stages, a first stage during which the electron distribution is progressively isotropized (for $t<\tau_{iso}$), and a second one during which the plasma is isotropic and expand with three degrees of freedom (for $t>\tau_{iso}$). As ν_0 increases, the duration of the first stage tends to zero. This is illustrated by Fig. 1(d) which displays the variation of τ_{iso} with ν_0, and indicates that the isotropization stage lasts less than $1/\omega_{pi0}$ for $\nu_0>60\omega_{pi0}$. For very high collision frequencies, the electron distribution function can therefore be considered as isotropic, whatever the initial temperatures are.

A similar analysis can be applied to the study of ion isotropization. In this case, we have to consider ion-ion and electron-ion collisions. Since the relaxation rate associated to ion-ion collisions is $(m_e/m_i)^{1/2}(T_{e0}/T_{i0})^{3/2}\nu_{iso}^{elec}/2$, the total relaxation rate for ion isotropization is

$$\nu_{iso}^{ion}=\left[1+\left(\frac{m_e}{m_i}\right)^{1/2}\left(\frac{T_{e0}}{T_{i0}}\right)^{3/2}\right]\nu_{iso}^{elec}/2.$$

This rate strongly depends on the ratio T_{e0}/T_{i0}. For $T_{i0}\ll T_{e0}$, the isotropization is mainly due to ion-ion collisions and $\nu_{iso}^{ion}>\nu_{iso}^{elec}$. In contrast, for $T_{i0}\gtrsim T_{e0}$, we have $\nu_{iso}^{ion}\approx\nu_{iso}^{elec}/2$. However, in all cases, the ion relaxation rate is of the same order or superior to the electron one. We can thus consider that the condition $\nu_0\gg\nu_0^{is}$ is sufficient to guarantee

that ion and electron distributions remain isotropic during all the expansion.

2. Electron-ion thermal equilibration

In Sec. II B 1, we assumed that electrons transfer their energy to ions through the charge separation field, and not through electron-ion collisions. This hypothesis is valid for low collision frequencies, as shown by Fig. 1(b), in which the ion temperature grows very little during the expansion. However, it is no more the case when the collision frequency is increased above few $100\omega_{pi0}$. This is illustrated by Fig. 1(c), in which the ion temperature grows from the beginning of the simulation up to $\tau_{eq} \approx 10\omega_{pi0}^{-1}$, where $T_e = T_i$.

The relaxation rate related to electron-ion thermal equilibration for $Z=1$ and $T_{i0} \lesssim T_{e0}$ is[22,25]

$$\nu_{eq} = \frac{8}{3\sqrt{\pi}} \frac{m_e}{m_i} \nu_o.$$

The equilibration rate is thus more than 10^3 smaller than the isotropization rate. Accordingly, Fig. 1(d) shows that for a given collision frequency, equilibration is much longer than isotropization. This confirms that energy transfers between electrons and ions are negligible for moderate collision frequencies.

Once electron and ion temperatures have been equilibrated, the energy remains equiparted if the energy transfer is fastest than the electron cooling down, i.e., if $\nu_{eq} \gg 1/\tau_e$. This leads to the relation

$$\nu_0 \gg \nu_0^{eq} = 0.2 \frac{m_i}{m_e} \frac{c_{s0}}{L}. \tag{3}$$

Note that in this case, we evaluate τ_e considering the ion acoustic velocity of the equilibrated plasma $c_s = c_{s0}/\sqrt{6}$. Substituting numerical values, we find that $T_e \approx T_i$ for all $t > \tau_{eq}$, if $\nu_0 \gg 20\omega_{pi0}$. This is illustrated by Fig. 1(c), obtained for $\nu_0 = 200\omega_{pi0}$, which shows that after the equilibration stage, electron and ion temperatures remain almost equal.

C. Limits of the Maxwellian and adiabatic regimes

In Sec. II B, we demonstrated that collisions can induce a large redistribution of the plasma energy between the longitudinal and transverse directions, as well as between ions and electrons. The influence of collisions on plasma expansion is, however, not limited to this redistribution, as they are also involved in heat transport. For moderate collision frequencies, they can in particular force the distribution functions to spatially homogeneous Maxwellian distributions, while for very high frequencies, they can prevent any heat transfer, leading to an adiabatic expansion.

1. Electron distribution Maxwellianization

In addition to their contribution to the isotropization of the electron distribution function, electron-electron collisions are actually also responsible for a redistribution of energy in the phase-space domain, that causes the kinetic distribution to relax to a Maxwellian. This process is governed by the energy exchange frequency ν_E which is the average time required for an electron to suffer a 100% change in energy. Indeed, an initially Maxwellian plasma remains Maxwellian during the expansion, if energy exchanges between electrons are significantly faster than the cooling-down, i.e., if $\nu_E \gg 1/\tau_e$. If we consider particles of root mean square velocity $v_{RMS} = (3k_B T_{e0}/m_e)^{1/2}$, we get $\nu_E \approx \nu_0$.[22,26] As a result, the Maxwellianization condition is

$$\nu_0 \gg \nu_0^{mx} = 0.4 \frac{c_{s0}}{L}. \tag{4}$$

For $L = L_0$, the plasma can, ergo, be considered as Maxwellian if $\nu_0 \gg 0.02\omega_{pi0}$.

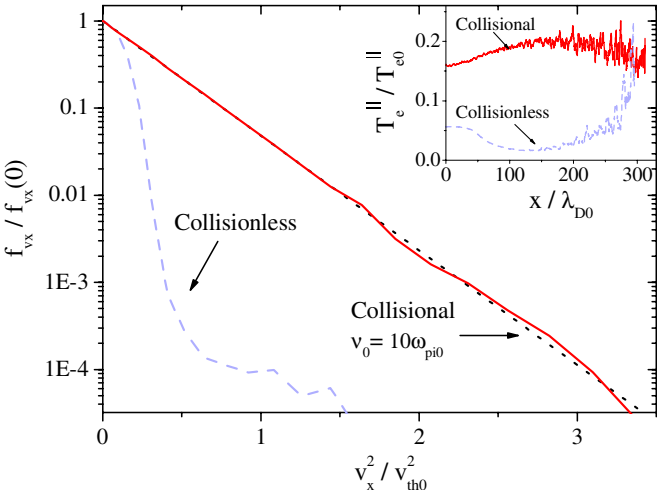

FIG. 2. (Color online) Maxwellianization of the electron distribution function. Main panel, distribution functions of the velocity in the expansion direction f_{vx}, for $\nu_0 = 0$ (collisionless plasma) and $\nu_0 = 10\omega_{pi0}$. These distributions are taken at the center of the foil ($x=0$), when $\omega_{pi0}t = 100$. The dotted line is the Maxwellian distribution function expected for $T_e^{\parallel} = 0.16 T_{e0}$. Inset, spatial variation of the local electron temperature, averaged over twenty meshes, with or without collisions.

Figure 2 displays electron distribution functions of the longitudinal velocity, obtained with or without collisions (i.e., for, respectively, $\nu_0 = 10\omega_{pi0}$ and $\nu_0 = 0$), for $T_{e0}^{\perp} = T_{e0}^{\parallel}$. We notice that electron-electron collisions strongly modify the distribution function, leading to an almost perfect Maxwellian distribution when $\nu_0 = 10\omega_{pi0}$. Besides, the inset of Fig. 2 shows that, in the collisionless case, the local electron temperature varies strongly because of kinetic effects,[21] whereas it is almost constant throughout the plasma in the collisional case. Energy exchanges between electrons are thus also responsible for a spatial homogenization of the temperature. The dotted line on the main panel represents the Maxwellian distribution corresponding to the temperature measured on the inset for $\nu_0 = 10\omega_{pi0}$. As expected, it reproduces almost perfectly the PIC distribution. This figure thus demonstrates that electron-electron collisions can efficiently force the distribution to relax to a homogeneous Maxwellian. We emphasize that the temperature homogenization is observed only for moderate collisions frequencies. Actually, for extremely high ν_0, the expansion becomes adiabatic.

TABLE I. Characteristic frequencies.

Regime	Expression	Value for $L=20\lambda_{D0}$
Isotropic	$\nu_0^{is} \approx 0.3\frac{c_{s0}}{L}$	$0.015\omega_{pi0}$
Maxwellian	$\nu_0^{mx} \approx 0.4\frac{c_{s0}}{L}$	$0.02\omega_{pi0}$
Equilibrated	$\nu_0^{eq} \approx 0.2\frac{m_i}{m_e}\frac{c_{s0}}{L}$	$20\omega_{pi0}$
Adiabatic	$\nu_0^{ad} \approx 6\frac{m_i}{m_e}\frac{c_{s0}}{L}$	$600\omega_{pi0}$

2. Heat transfer characteristic time

An adiabatic process is characterized by an absence of heat transfer. In order to determine the collision frequency required to suppress the heat transport, we first consider the 1D heat equation

$$C_v\frac{\partial T_e}{\partial t} - \frac{\partial}{\partial x}\kappa\frac{\partial T_e}{\partial x} = 0, \tag{5}$$

where C_v is the heat capacity at constant volume and κ the thermal conductivity. In the highly collisional case, the plasma is isotropic and $C_v=3/2n_ek_B$. Besides, assuming that the electron mean free path is somewhat smaller than the temperature gradient scale length $L_T=T_e/\nabla T_e$, we can use the Spitzer–Härm expression[27] for κ, that is for $Z=1$,

$$\kappa \approx 4\frac{n_ek_B^2T_e}{m_e\nu_0}. \tag{6}$$

The heat transfer characteristic time $\tau_h=T_e(\partial T_e/\partial t)^{-1}$, is then derived from Eq. (5)

$$C_v\frac{T_e}{\tau_h} \approx \frac{7}{2}\kappa\frac{T_e}{L_T^2} \Leftrightarrow \tau_h \approx 0.1\frac{\nu_0 L_T^2}{k_BT_e/m_e}. \tag{7}$$

Finally, assuming that $L_T \approx L$ and that the plasma is equilibrated $(T_e=T_i=T_0)$, the adiabaticity condition $\tau_h \gg \tau_e = (3/2\sqrt{5})L/c_{s0}$ (see Sec. IV), writes

$$\nu_0 \gg \nu_0^{ad} = 6\frac{m_i}{m_e}\frac{c_{s0}}{L}. \tag{8}$$

Substituting numerical values, we obtain $\nu_0^{ad} \approx 600\omega_{pi0}$.

This value is reported, with the other characteristic frequencies, in Table I. It emphasizes that, in the adiabatic regime, the plasma is isotropized and equilibrated, and justifies so the assumptions made before. Table I also helps to identify two regimes of interest, namely the Maxwellian-isotropic and nonequilibrated regime for $0.02\omega_{pi0} \ll \nu_0 < 20\omega_{pi0}$, and the equilibrated-adiabatic regime for $\nu_0 \gg 600\omega_{pi0}$. Note that to enter one of these regimes, the basic collision frequency ν_0 has to be significantly greater than the corresponding characteristic frequency. These frequencies have actually been calculated for particles of velocity $(2k_BT_0/m_e)^{1/2}$, but the collision frequencies of suprathermal particles are much lower. For instance, the collision frequency of an electron of velocity $6.5(k_BT_0/m_e)^{1/2}$ is about $\nu_0/100$. The characteristic collision frequencies corresponding to such an electron are thus 100 times larger than the mean values reported in Table I.

III. MAXWELLIAN-ISOTROPIC REGIME

In this section, we focus on the Maxwellian-isotropic regime of expansion. We first introduce a slightly modified version of the code described in Ref. 12. This code is then used to interpret results from PIC simulations, in which electron-ion and ion-ion collisions are neglected. We finally discuss a more realistic case, where electron-ion and ion-ion collisions are taken into account.

A. Hybrid code

The code used in this section to analyze PIC results, is a hybrid Lagrangian code which describes the expansion of a plasma slab with cold ions, initially at rest, and sharp boundaries. The electron density is modeled by a Maxwell–Boltzmann distribution. For $t>0$, electrons are assumed to remain in equilibrium with the electric potential Φ satisfying the Poisson equation, while the ion expansion is described by the equations of motion. Besides, the evolution in time of the electron temperature is determined by the energy conservation law

$$\frac{dU_e}{dt} = -k_BT_e\int_{-\infty}^{\infty} n_e\frac{\partial v_e}{\partial x}dx, \tag{9}$$

where $U_e=1/2N_{e0}k_BT_e$ is the total electron thermal energy, and $N_{e0}=2n_{e0}L$ the total number of electrons. Due to the symmetry of the plasma, the boundary conditions are, for any time, $E(\pm\infty)=0$, $E(x=0)=0$, and $v_i(x=0)=0$, where E is the electric field, v_i is the ion velocity, and $x=0$ is the coordinate of the foil center.

The code described in Ref. 12 models the expansion of a purely 1D plasma, while in the present case collisions drive energy exchanges between the longitudinal and transverse momenta. To take into account these three degrees of freedom, we assumed that the electron energy is, at any time, equally distributed along each direction, that is $U_e = 3/2N_{e0}k_BT_e$ with $T_e^{\perp}=T_e^{\parallel}=T_e$, and modified accordingly the energy conservation law. This assumption is justified if the isotropization time is much shorter than the expansion characteristic time, that is if $\nu_0 \gg \nu_0^{is}$. However, even when this condition is satisfied, the code thus modified does not fully describe the effect of collisions in the Maxwellian-isotropic regime. Indeed, it does not include any collisional energy transfer between ions and electrons. Such transfers are however not totally negligible, when ν_0 becomes of the order of several ω_{pi0}. Modeling these collisions would necessitate substantial changes to the code. Nevertheless, even in its present state, this code can give some insight into the Maxwellian-isotropic regime of expansion.

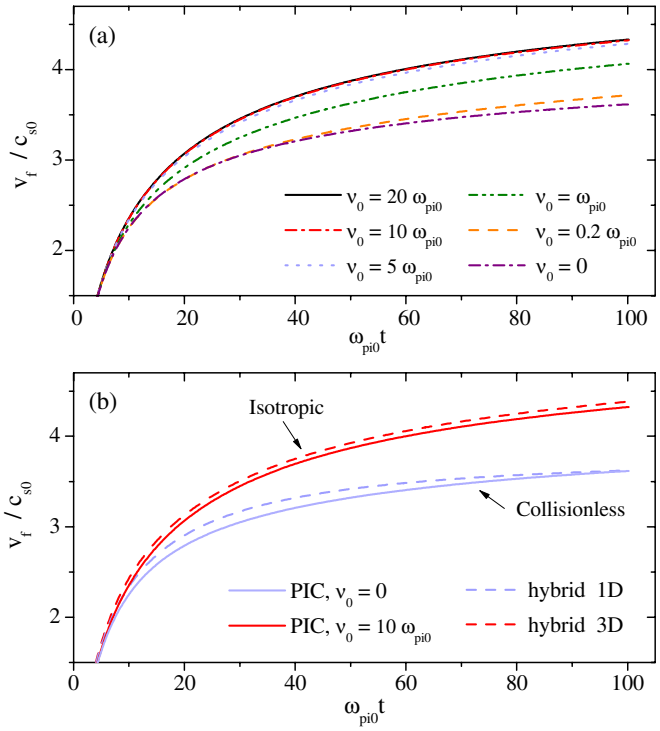

FIG. 3. (Color online) Identification of the Maxwellian-isotropic regime of expansion. (a) Dependence on time of the ion front velocity, for collision frequencies $0 \leq \nu_0 \leq 20\omega_{pi0}$. (b) Comparisons of the ion front velocities calculated using the hybrid code or the PIC code. The two curves associated with the hybrid code, labeled "hybrid 1D" and "hybrid 3D" correspond, respectively, to the 1D version of the code described in Ref. 12, and to the isotropic version presented in Sec. III A. The longitudinal temperature $T_e^{\parallel}$ is the same in both cases.

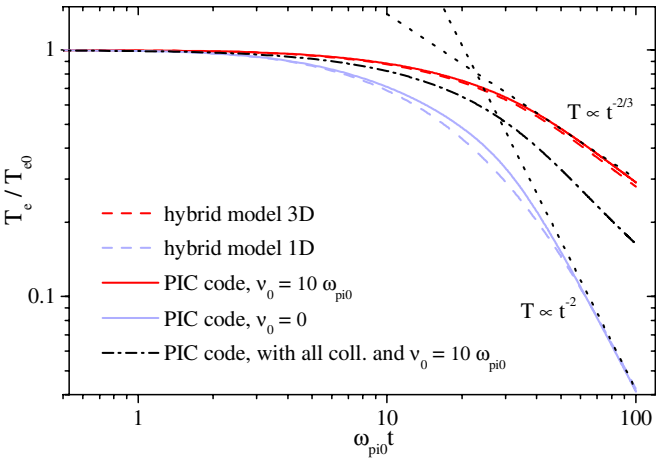

FIG. 4. (Color online) Time dependence of the electron mean temperature in the collisionless and isotropic regimes. Solid lines correspond to the PIC code, dashed lines to the hybrid model and dotted lines to the asymptotes $T \propto t^{-2/3}$ and $T \propto t^{-2}$. The result of a PIC simulation including all Coulomb collisions is also plotted (dash-dotted line).

B. Influence of electron-electron collisions only

At first, we performed PIC simulations with electron-electron collisions only. We emphasize that these simulations do not correspond to realistic conditions. Indeed, even when ions and electrons exchange little energy, electron-ion collisions contribute to the isotropization rate (see Sec. II B 1). This study is anyway useful, to isolate the effect of isotropization and Maxwellianization on the expansion.

Figure 3(a) shows, for various collision frequencies, the time dependence of the ion front velocity $v_f(t)$, obtained from PIC simulations. In these simulations, the longitudinal and transverse temperatures are initially equal. We observe that v_f increases with ν_0, and saturates around $\nu_0 \approx 10\omega_{pi0}$. We notice also that the influence of collisions on the expansion is almost negligible for $\nu_0 < 0.2\omega_{pi0}$. This result seems inconsistent with Fig. 1(b), where the effect of collisions appears to be strong for $\nu_0 = 0.2\omega_{pi0}$. This discrepancy is only apparent. Up to now, we have assumed that the collision frequency ν_0 is constant in time, but it actually increases as the electron temperature goes down. The frequency ν_0 can thus be too low to counterbalance the energy transfer from electrons to ions, at the beginning of the expansion, but sufficiently high to do it, once the plasma has cooled down. For instance, in the case of Fig. 3(a), we observed that, for $\nu_0 = 0.2\omega_{pi0}$, the ratio $T_e^{\perp}/T_e^{\parallel}$ increases while $t \lesssim 40\omega_{pi0}$. This means that collisions do not affect significantly the expansion before this time. This analysis is consistent with Fig. 3(a), in which the function $v_f(t)$ for $\nu_0 = 0.2\omega_{pi0}$, do not differ from the collisionless case before $t \approx 40\omega_{pi0}$. In Fig. 1(b), the isotropization seems to be efficient, because $T_e^{\perp}$ is of the same order than $T_e^{\parallel}$, for $t \geq \tau_{iso}$. However, in the case of Fig. 1(b) also, $T_e^{\perp}/T_e^{\parallel}$ increases while $t \lesssim 40\omega_{pi0}$, and the expansion enters the isotropic regime only after this time. There is hence no contradiction between Figs. 1(b) and 3(a).

The saturation observed in Fig. 3(a) indicates that, when $\nu_0 \gtrsim 10\omega_{pi0}$, the isotropization is faster than the electron cooling, so much so that the plasma remains isotropic during the whole expansion. Figure 3(b) compares the curves $v_f(t)$, obtained from PIC simulations for $\nu_0 = 10\omega_{pi0}$ and $\nu_0 = 0$ (collisionless case), with the ones resulting from hybrid simulations performed using 1D or three-dimensional (3D) electron temperature repartitions. The agreement between the two models is quite satisfactory. In the collisionless regime, the curves resulting from the hybrid an PIC codes have, however, somewhat different behaviors. This comes from electron kinetic effects which force the electron distribution function to deviate from a Maxwellian (see Fig. 2 and Ref. 21). Such effects are indeed not described by the hybrid code. In the collisional case, both curves have the same shape, as collisions maintain the distribution Maxwellian, but their amplitudes are slightly different. This discrepancy arises from the difficulty of evaluating precisely v_f. Indeed, because the density tends to zero at the ion front, its position and velocity depend on the discretization of the density function, that is in the context of PIC simulations, on the number of particles in each cell. Be that as it may, the differences between the two codes are definitely small.

A similar agreement between both codes is obtained in Fig. 4 which displays electron temperatures as a function of time. The long-time asymptotic behavior of T_e is derived from Eq. (9), assuming $v_e \approx x/t$.[12] Doing so, we get $dT_e/dt = -aT_e/t$, resulting in $T_e \propto t^{-a}$, with $a=2$ in the collisionless regime and $a=2/3$ in the isotropic case. Electron cooling is thus much slower in the isotropic regime. Accordingly, in Fig. 3(b), the slope of $v_f(t)$ at long time is steeper for ν_0

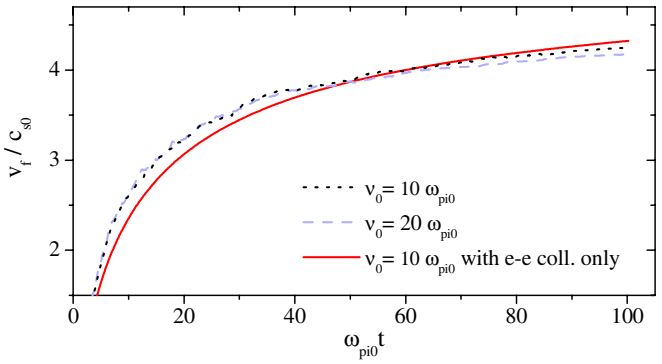

FIG. 5. (Color online) Ion front velocity as a function of time, with or without electron-ion and ion-ion collisions.

$=10\omega_{\mathrm{pi0}}$ than for $\nu_0=0$. Note that we verified with the hybrid code, that though the acceleration is slower, $v_f(t)$ converges, in the collisional case, to almost the same maximal velocity than in the case of a collisionless plasma with $T_0^{\parallel}=6T_0$ and $T_0^{\perp}=0$.

C. Simulations with all type of collisions

Figures 3 and 4 demonstrate that electron-electron collisions cause the plasma to expand with three degrees of freedom when $\nu_0 \gtrsim 10\omega_{\mathrm{pi0}}$, and that this process is accurately described by a simple expansion model. However, electron-ion and ion-ion collisions cannot be rigorously neglected. Indeed, Figs. 4 and 5 show that these collisions affect the time dependence of both the electron temperature and the ion front velocity. In particular, we notice that, when all collisions are considered, v_f grows faster at early times, and more slowly at late times. This faster increase arises from the fact that, while $t<\tau_{\mathrm{eq}}$, electrons transfer a part of their energy to ions, through electron-ion collisions. Accordingly, the electron temperature diminishes quicker in this case (see Fig. 4). The gentle ion acceleration observed at long times, is then a consequence of this lower temperature. One can note that because of ion-ion collisions, the curves $v_f(t)$ are noisier when all collisions are taken into account.

Figure 5 also illustrates that the deformation of $v_f(t)$ is slightly amplified by an increase of ν_0. This was expected as the energy transfer between ions and electrons grows with the equilibration rate $\nu_{\mathrm{eq}} \propto \nu_0$. These variations are, however, relatively small, so much so that the hybrid model provides an acceptable approximation of $v_f(t)$. To conclude this section, we emphasize that, in a laser-plasma experiment, the laser does not generally heat isotropically the plasma. As a consequence, the isotropic regime described here can be preceded by a transient stage (for $t<\tau_{\mathrm{iso}}$), during which the electron distribution is isotropized.

IV. ADIABATIC REGIME

When the collision frequency ν_0 significantly exceeds ν_0^{ad}, the expansion ceases to be isothermal and becomes adiabatic. As $\nu_0^{\mathrm{ad}}>\nu_0^{\mathrm{eq}}$, we assume in this section that ion and electron distributions are initially equilibrated, i.e., $T_{e0}=T_{i0}=T_0$.

We begin our analysis by deriving a self-similar solution for the adiabatic expansion.[28] The continuity and momentum equations for the ion fluid are

$$\frac{\partial n_i}{\partial t}+\frac{\partial}{\partial x}(n_i v_i)=0, \tag{10}$$

$$m_i n_i\left(\frac{\partial v_i}{\partial t}+v_i\frac{\partial v_i}{\partial x}\right)=Zn_i eE-\frac{\partial p_i}{\partial x}+R_i, \tag{11}$$

where p_i is the ion pressure, E is the electric field, and R_i is a term that describes electron-ion collisions. Similarly, neglecting electron inertia, the electron momentum equation writes

$$0=-n_e eE-\partial p_e/\partial x+R_e, \tag{12}$$

where p_e is the electron pressure and $R_e=-R_i$. Combining Eqs. (11) and (12), we get

$$m_i n_i\left(\frac{\partial v_i}{\partial t}+v_i\frac{\partial v_i}{\partial x}\right)=(Zn_i-n_e)eE-\frac{\partial p_i}{\partial x}-\frac{\partial p_e}{\partial x}. \tag{13}$$

Then, we assume that $n_e=Zn_i$ which is a good approximation away from the ion front, and use the self similar parameter $\xi=x/t$ to get from Eqs. (10) and (13)

$$(v_i-\xi)\frac{dn_i}{d\xi}+n_i\frac{dv_i}{d\xi}=0, \tag{14}$$

$$(v_i-\xi)\frac{dv_i}{d\xi}=-\frac{1}{n_i m_i}\frac{d}{d\xi}(p_i+p_e). \tag{15}$$

To go further, we consider that both fluids are ideal gases, and use adiabatic equations of state to obtain expressions for the pressures. In the case of ions, this leads to

$$p_i=n_{i0}k_B T_0(n_i/n_{i0})^{\gamma}, \tag{16}$$

where $\gamma=5/3$ is the adiabatic index for a gas with three degrees of freedom. Moreover, we assume that the plasma remains equilibrated during all the expansion. Thus, we have $p_e=Zp_i$ and Eq. (15) becomes

$$(v_i-\xi)\frac{dv_i}{d\xi}=-\frac{c_0^2}{n_{i0}}\left(\frac{n_i}{n_{i0}}\right)^{\gamma-1}\frac{dn_i}{d\xi}, \tag{17}$$

where $c_0=c_{s0}\sqrt{\gamma(1+Z)/6Z}$. Eliminating $dv_i/d\xi$ and $dn_i/d\xi$ from Eqs. (14) and (17) yields,

$$v_i=\xi\pm c_0(n_i/n_{i0})^{(\gamma-1)/2}. \tag{18}$$

Finally, we substitute the derivative of Eq. (18) into Eq. (14), and integrate the equation obtained to get

$$n_i^{\mathrm{ad}}(\xi)=n_{i0}\left(\frac{2}{\gamma+1}-\frac{\gamma-1}{\gamma+1}\frac{\xi}{c_0}\right)^{2/\gamma-1}, \tag{19}$$

$$v_i^{\mathrm{ad}}(\xi)=\frac{2}{\gamma+1}(\xi+c_0). \tag{20}$$

Note that we have chosen the positive sign in Eq. (18) to get a density that decreases when ξ increases. The constant of integration has been determined using the fact that, in the unperturbed plasma, $v_i^{\mathrm{ad}}=0$ and $n_i=n_{i0}$. For that reason, these

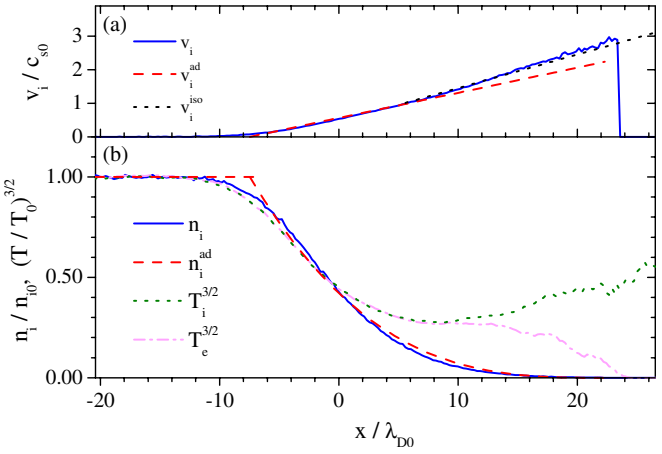

FIG. 6. (Color online) Adiabatic expansion of a plasma foil, for $\nu_0 = 2000\omega_{pi0}$. (a) Ion velocity as a function of the distance to the initial position of the plasma surface x. The solid line corresponds to the PIC code, the dashed line to the adiabatic self-similar model and the dotted line to the isotherm self-similar model. (b) Ion density, and electron/ion temperatures raised to the power 3/2, as a function of x. The temperatures are averaged over twenty meshes. In the adiabatic part of the plasma $n_i/n_{i0}=(T/T_0)^{3/2}$.

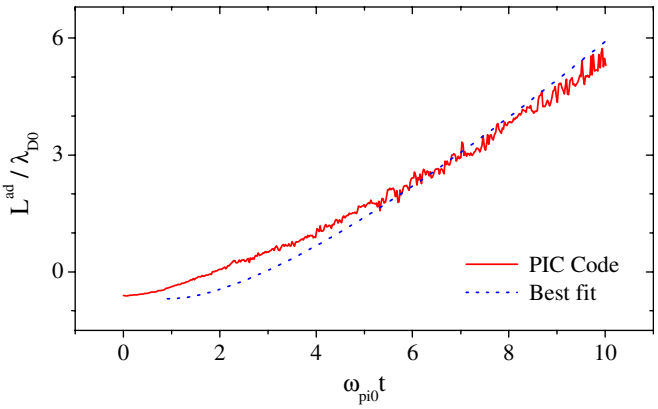

FIG. 7. (Color online) Limit of the adiabatic region as a function of time, for $\nu_0=2000\omega_{pi0}$. The value of x_{ad} extracted from the PIC code is the coordinate of the point where $n_i/n_{i0}=0.5(T_i/T_{i0})^{3/2}$. The fit corresponds to the function $x_{ad}(t)=c_0t[3-4(t_{ad}/t)^{1/4}]$ with $t_{ad}=0.9\omega_{pi0}^{-1}$.

equations do not fully describe the expansion, after the rarefaction wave has reached the center of the plasma slab.

The density n_i^{ad} and the velocity v_i^{ad}, calculated at $\omega_{pi0}t=10$ for $Z=1$, are plotted in Fig. 6, together with PIC results obtained for $\nu_0=2000\omega_{pi0}$. We observe that the plasma behaves differently, depending on whether $x \lesssim x_{ad} \approx 4\lambda_{D0}$, or $x \gtrsim x_{ad}$. In the part $x \lesssim x_{ad}$, the expansion is adiabatic with $n_i/n_{i0} \approx (T/T_0)^{\gamma-1}$. Accordingly, the self-similar adiabatic model reproduces well the velocity and density profiles given by the PIC code. In contrast, in the part $x \gtrsim x_{ad}$, the equation of state is no more adiabatic, and the temperatures remain almost constant as n_i decreases. We remark, however, that the plasma is not equilibrated in the neighborhood of the ion front, as the collision frequency $\nu \propto n_e/T_e^{3/2}$ decreases when x increases. We observe also that v_i deviates significantly from v_i^{ad} for $x \gtrsim x_{ad}$. In this part of the plasma, v_i is actually more satisfactorily fitted by the self-similar isothermal velocity $v_i^{iso}=v_i^{ad}(x_{ad}/t)+(x-x_{ad})/t$.[11]

To explain these observations, the analysis of the Sec. II has to be refined; this analysis is indeed not valid at the beginning of the expansion, since we took $L_T \approx L$ and $\tau_e \propto L/c_{s0}$. To this end, we assume that the plasma is adiabatic, and we investigate the conditions for which this hypothesis ceases to be true. From Eqs. (16) and (19), in which we have substituted $\xi=2c_0/(\gamma-1)-z/t$ and $\gamma=5/3$, we get $T=T_0(z/4c_ot)^2$. Then from Eq. (7), we obtain the heat transport characteristic time

$$\tau_h \approx 0.5 \frac{\nu_0 (c_0 t)^2}{k_B T_0 / m_e}. \tag{21}$$

This equation shows that τ_h increases in time, as long as the rarefaction wave has not reached the center of the plasma slab. To determine the limit of the adiabatic regime, this time has to be compared to the cooling characteristic time $\tau_e = T|\partial T/\partial t|^{-1} = t/2$. Doing so, we find that the expansion cannot be adiabatic as long as

$$t \lesssim t_{ad} = 0.3 \frac{m_i}{m_e} \nu_0^{-1}. \tag{22}$$

Substituting numerical values, we obtain, for $\nu_0=2000\omega_{pi0}$ and $t_{ad} \approx 0.3\omega_{pi0}^{-1}$.

Before t_{ad}, the plasma expands as an isotropic Maxwellian plasma. For $t>t_{ad}$, the plasma is divided in two regions which expand differently. The region of the plasma which has started to expand before t_{ad} continues to expand nonadiabatically, whereas the region which has started to expand only after t_{ad} undergoes an adiabatic expansion. At $t=t_{ad}$, we have $x_{ad0} \approx -c_0 t_{ad}$. Then, for $t \geq t_{ad}$, $x_{ad}(t)$ can be evaluated, exploiting the fact that the quantity of matter in the adiabatic part is conserved, that is $\int_{-c_0 t}^{x_{ad}(t)} n_i(x)dx = n_{i0}c_0(t-t_{ad})$. Using Eq. (19), this conservation law results, for $L/c_0 \geq t \geq t_{ad}$, in

$$x_{ad}(t) = c_0 t[3 - 4(t_{ad}/t)^{1/4}]. \tag{23}$$

We remark that, in the limit $t \gg t_{ad}$, $x_{ad}(t) \approx 3c_0 t$. This means that, at long times, the boundary of the adiabatic region corresponds to the position of the ion front predicted by the self-similar adiabatic model [see Eq. (19)]. In addition, we notice that the plasma tends to be fully adiabatic as $\nu_0 \to \infty$. We emphasize also that, for any collision frequency ν_0, one can find plasma slab half-lengths L, such that $L/c_0 > t_{ad}(\nu_0)$. This means that the inner part of a very thick plasma always expands adiabatically.

According to Eqs. (22) and (23), $x_{ad}(10\omega_{pi0}) \approx 10\lambda_{D0}$. This value is inconsistent with Fig. 6, where the expansion is observed to be approximately adiabatic up to $x \approx 4\lambda_{D0}$. One possible reason for this discrepancy is that ν_0 has been calculated for particles of mean velocities, while the heat transport is mainly carried out by the fastest electrons. In order to evaluate the effective duration of the fully nonadiabatic stage, we looked for the value of t_{ad} which best fit the function $x_{ad}^{PIC}(t)$ obtained from the PIC simulation. For this analysis, we define $x_{ad}^{PIC}(t)$ as the point where the temperature raised to the power 3/2 becomes twice as big as the density. Figure 7 shows that the agreement between $x_{ad}^{PIC}(t)$ and the analytic function $x_{ad}(t)$ is quite satisfactory for $t_{ad}=0.9\omega_{pi0}^{-1}$. This time corresponds to a collision frequency approximately

three times smaller than ν_0, that is to a mean velocity of about $2(k_B T_e/m_e)^{1/2}$. Note that these values are just rough estimates, as the criterion use to determine $x_{ad}^{PIC}(t)$ is arbitrary.

V. DISCUSSION

In Sec. II, we have identified two regimes of collisional plasma expansion: the Maxwellian-isotropic regime which is numerically observed for $10 \lesssim \nu_0/\omega_{pi0} \ll 600$, and the partly adiabatic regime which required $\nu_0/\omega_{pi0} \gg 600$. Up to now, we have, however, not specified the physical parameters leading to such collision frequencies. If we consider a fully ionized aluminum target of half-thickness L_0, with $n_{e0}=7.8 \times 10^{23}$ cm^{-3}, and use the Lee and More expression for $\ln \Lambda$,[23] we find that a collision frequency $\nu_0=10\omega_{pi0}$ corresponds to an electron temperature $T_{e0} \approx 140$ eV, and that $\nu_0=2000\omega_{pi0}$ is obtained for $T_{e0} \approx 3$ eV. However, according to Ref. 23, the electron conductivity model of Spitzer and Härm does not apply to temperatures below 10 eV. For $T_{e0}=3$ eV, this model actually underestimates the thermal conductivity by a factor of almost 10. As a consequence, still lower temperatures are necessary to reach the adiabatic regime in the considered conditions.

Obviously, electron temperatures required to observe the collisional regimes of expansion are much lower than those related to laser-plasma ion acceleration which are generally of several hundreds of keV. The present study could, however, be relevant to other kind of experiments. An important example is the expansion of warm dense matter, heated isochoricly by ultrafast proton beams.[29–31] Electron temperatures obtained in this way are actually about few tens of eV. In Ref. 29, for instance, a 10 μm thick Al target is heated up to 23 eV. In this case, the basic collision frequency is about $100\omega_{pi0}$, $L \approx 10^5 \lambda_{D0}$, and $\nu_0^{ad} \approx 0.1\omega_{pi0}$. The expansion is thus expected to be partly adiabatic, with a first Maxwellian-isotropic stage which lasts $t_{ad} \approx 18\omega_{pi0}^{-1}$, and is then followed by a second stage, during which two $x_{ad0} \approx 1$ nm thick layers on both sides of the plasma go on expanding in the Maxwellian-isotropic regime, while the rest of the plasma expands adiabatically.

This illustrates how Coulomb collisions can affect the expansion of a 1D plasma into a vacuum. We emphasize that in two or three space dimensions, other effects come into play. As an example, it is shown in Ref. 32 that electron-ion collisions near the target surface can contribute to the emittance growth of laser-accelerated proton beams. Lastly, we stress that electromagnetic instabilities which are another potential source of coupling between the transverse and longitudinal directions, could lead to effects similar to those described in Sec. III.

ACKNOWLEDGMENTS

This work was partly supported by Agence Nationale de la Recherche, Project No. ANR-06-BLAN-0392.

[1] E. L. Clark, K. Krushelnick, J. R. Davies, M. Zepf, M. Tatarakis, F. N. Beg, A. Machacek, P. A. Norreys, M. I. K. Santala, I. Watts, and A. E. Dangor, Phys. Rev. Lett. **84**, 670 (2000).
[2] R. A. Snavely, M. H. Key, S. P. Hatchett, T. E. Cowan, M. Roth, T. W. Phillips, M. A. Stoyer, E. A. Henry, T. C. Sangster, M. S. Singh, S. C. Wilks, A. MacKinnon, A. Offenberger, D. M. Pennington, K. Yasuike, A. B. Langdon, B. F. Lasinski, J. Johnson, M. D. Perry, and E. M. Campbell, Phys. Rev. Lett. **85**, 2945 (2000).
[3] M. Borghesi, J. Fuchs, S. V. Bulanov, A. J. Mackinnon, P. K. Patel, and M. Roth, Fusion Sci. Technol. **49**, 412 (2006).
[4] J. Fuchs, P. Antici, E. D'Humières, E. Lefebvre, M. Borghesi, E. Brambrink, C. A. Cecchetti, M. Kaluza, V. Malka, M. Manclossi, S. Meyroneinc, P. Mora, J. Schreiber, T. Toncian, H. Pépin, and P. Audebert, Nat. Phys. **2**, 48 (2006).
[5] L. Robson, P. T. Simpson, R. J. Clarke, K. W. D. Ledingham, F. Lindau, O. Lundh, T. McCanny, P. Mora, D. Neely, C.-G. Wahlström, M. Zepf, and P. McKenna, Nat. Phys. **3**, 58 (2007).
[6] T. Ceccotti, A. Lévy, H. Popescu, F. Réau, P. D'Oliveira, P. Monot, J.-P. Geindre, E. Lefebvre, and P. Martin, Phys. Rev. Lett. **99**, 185002 (2007).
[7] S. P. Hatchett, C. G. Brown, T. E. Cowan, E. A. Henry, J. S. Johnson, M. H. Key, J. A. Koch, A. B. Langdon, B. F. Lasinski, R. W. Lee, A. MacKinnon, D. M. Pennington, M. D. Perry, T. W. Phillips, M. Roth, T. C. Sangster, M. S. Singh, R. A. Snavely, M. A. Stoyer, S. C. Wilks, and K. Yasuike, Phys. Plasmas **7**, 2076 (2000).
[8] J. Denavit, Phys. Rev. Lett. **69**, 3052 (1992).
[9] L. O. Silva, M. Marti, J. R. Davies, R. A. Fonseca, C. Ren, F. S. Tsung, and W. B. Mori, Phys. Rev. Lett. **92**, 015002 (2004).
[10] T. Esirkepov, M. Borghesi, S. V. Bulanov, G. Mourou, and T. Tajima, Phys. Rev. Lett. **92**, 175003 (2004).
[11] A. V. Gurevich, L. V. Pariĭskaya, and L. P. Pitaevskii, Zh. Eksp. Teor. Fiz. **49**, 647 (1965).
[12] P. Mora, Phys. Rev. E **72**, 056401 (2005).
[13] J. E. Crow, P. L. Auer, and J. E. Allen, J. Plasma Phys. **14**, 65 (1975).
[14] J. S. Pearlman and R. L. Morse, Phys. Rev. Lett. **40**, 1652 (1978).
[15] J. Denavit, Phys. Fluids **22**, 1384 (1979).
[16] P. Mora and R. Pellat, Phys. Fluids **22**, 2300 (1979).
[17] A. V. Gurevich and A. P. Meshcherkin, Zh. Eksp. Teor. Fiz. **80**, 1810 (1981).
[18] M. A. True, J. R. Albritton, and E. A. Williams, Phys. Fluids **24**, 1885 (1981).
[19] Y. Kishimoto, K. Mima, T. Watanabe, and K. Nishikawa, Phys. Fluids **26**, 2308 (1983).
[20] P. Mora, Phys. Rev. Lett. **90**, 185002 (2003).
[21] T. Grismayer, P. Mora, J. C. Adam, and A. Héron, Phys. Rev. E **77**, 066407 (2008); P. Mora and T. Grismayer, Phys. Rev. Lett. **102**, 145001 (2009).
[22] L. Spitzer, *Physics of Fully Ionized Gases* (Interscience, New York, 1956).
[23] Y. T. Lee and R. M. More, Phys. Fluids **27**, 1273 (1984).
[24] K. Nanbu, Phys. Rev. E **55**, 4642 (1997).
[25] T. Takizuka and H. Abe, J. Comput. Phys. **25**, 205 (1977).
[26] W. M. MacDonald, M. N. Rosenbluth, and W. Chuck, Phys. Rev. **107**, 350 (1957).
[27] L. Spitzer and R. Härm, Phys. Rev. **89**, 977 (1953).
[28] L. D. Landau and E. M. Lifshitz, *Fluid Mechanics* (Addison-Wesley, Reading, MA, 1959).
[29] P. K. Patel, A. J. MacKinnon, M. H. Key, T. E. Cowan, M. E. Foord, M. Allen, D. F. Price, H. Ruhl, P. T. Springer, and R. Stephens, Phys. Rev. Lett. **91**, 125004 (2003).
[30] E. Brambrink, T. Schlegel, G. Malka, K. U. Amthor, M. M. Aléonard, G. Claverie, M. Gerbaux, F. Gobet, F. Hannachi, V. Méot, P. Morel, P. Nicolai, J. N. Scheurer, M. Tarisien, V. Tikhonchuk, and P. Audebert, Phys. Rev. E **75**, 065401 (2007).
[31] G. M. Dyer, A. C. Bernstein, B. I. Cho, J. Osterholz, W. Grigsby, A. Dalton, R. Shepherd, Y. Ping, H. Chen, K. Widmann, and T. Ditmire, Phys. Rev. Lett. **101**, 015002 (2008).
[32] A. J. Kemp, J. Fuchs, Y. Sentoku, V. Sotnikov, M. Bakeman, P. Antici, and T. E. Cowan, Phys. Rev. E **75**, 056401 (2007).